11-1-2002

High frequency-bandwidth optical technique to measure thermal elongation time responses of near-field scanning optical microscopy probes

Andres H. La Rosa
andres@pdx.edu

B. Biehler

Citation Details

B. Biehler and A. H. La Rosa, "High frequency-bandwidth optical technique to measure thermal elongation time responses of near-field scanning optical microscopy (NSOM) probes," Rev. Sci. Instrum. 73, 3837-40 (2002).

High frequency-bandwidth optical technique to measure thermal elongation time responses of near-field scanning optical microscopy probes

B. Biehler and A. H. La Rosa[a)]
Department of Physics, Portland State University, Portland, Oregon 97207

(Received 17 May 2002; accepted 27 July 2002)

A near-field scanning optical microscopy (NSOM) probe elongates when light is coupled into it. The time response of this thermal process is measured here by a new optical technique that exploits the typical flat-apex morphology of the probe as a mirror in a Fabry–Perot type cavity. Pulsed laser light is coupled into the probe to heat up the tip, while another continuous wave laser serves to monitor the elongation from the interference pattern established by the reflections from the flat-apex probe and a semitransparent metal-coated flat sample. A quarter wave plate is introduced into the interferometer optical path in order to maximize the signal to noise level, thus allowing the elongation of the tip to be monitored in real time. This optical technique, unlike other methods based on electronic feedback response, avoids limited frequency bandwidth restrictions. We have measured response time constants of 500 and 40 μs. The technique presented here will help determine the power levels, operating probe-sample distance, and pulse repetition rate requirements for safe operation of NSOM instrumentation. In addition to NSOM, the instrumentation described in this article could also impact other areas that require large working range, accuracy, and high-speed response. [DOI: 10.1063/1.1510548]

I. INTRODUCTION

The potential to implement optical metrology at mesoscopic scale has sparked much interest in the novel near-field scanning optical microscopy (NSOM) technique.[1,2] Its superior lateral resolution, when compared to conventional (far-field) optical microscopy, is typically obtained by channeling optical radiation through a metal-coated tapered fiber that has a subwavelength dimension aperture at its apex. NSOM has been applied in diverse fields[3] ranging from high-density data storage,[4,5] light pulse propagation in photonic structures,[6] and charge carrier dynamic studies in semiconductors,[7,8] to imaging biological samples.[9,10] It has also proved single molecule sensitivity at room temperature.[3,11] Presently, there is much interest in improving NSOM probes throughput efficiencies to enable widespread use of NSOM in areas that require high intensity light sources.[2,12,13]

One of the primary limitations in metal-coated tapered probes is the limited power (10^{11} photons/s or ~50 nW) that can effectively be coupled into a subwavelength aperture probe, in that a large quantity of 1 mW level input power is either reflected back through the fiber or deposited as heat in a region close to the probe apex. Unfortunately, attempts to increase the probe's optical throughput by increasing the input power can lead to irreversible harm to the probe morphology, mainly due to the probe's poor heat dissipation efficiency.[14] The limited channels for heat dissipation also leads to steady state temperatures above ambient in the probe apex (~100 K/mW) when moderate input power levels are used, which causes a variety of effects in the probe performance. In this article we focus on the probe's axial elongation effect caused by thermal phenomena. This aspect is very important in near-field optical imaging since the coupling of the evanescent fields from the probe into the sample is expected to be very sensitive to the probe-sample distance. Furthermore, precise evaluation of the probe's thermal elongation becomes critical in time-resolved NSOM applications that require pulsed or amplitude modulated input power, since the thermal-driven periodic contraction and elongation of the metal-coated probe can produce artifacts in the near-field images. However, there is a lack of quantitative information about the magnitude of this contraction/elongation thermal effect, particularly when a short-duration pulse or a high frequency amplitude modulated input power is used. Advances in probe characterization techniques with high frequency bandwidth (capable to measure the fastest time responses involved in probe elongations) will be very beneficial in evaluating the magnitude of this thermal effect. On the other hand, thermal probe elongation could be turned to our advantage by using NSOM probes as indenters to locally modify soft films in high-density data storage applications. Evaluation of the potential and ultimate success of these applications, when compared to other recently proposed data storage methods,[15] will require to harness the NSOM probe's writing rate capability.

In short, to expand the potential applications of NSOM, it is important to quantify the time scale(s) at which NSOM probe axial elongations occur when exposed to pulsed light, which is the subject of this article. Here, we introduce a new technique based on optical interference that will allow the measurement of thermal time constants without frequency bandwidth restrictions.

a)Electronic mail: andres@pdx.edu

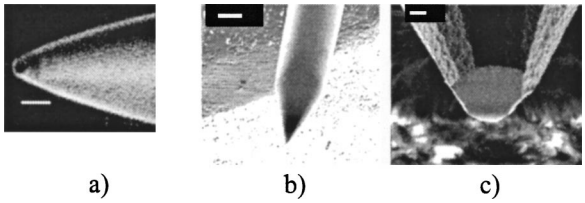

FIG. 1. Characteristic flat apex morphologies. (a) Probe fabricated using the heat-pulling method. (b) Fiber tapered by chemical etching. (c) Fully metal-coated probe sectioned by a focused ion beam. Scales bars are 1, 50, and 2 μm, respectively.

II. PROBE'S AXIAL ELONGATION MEASUREMENT

Previous measurements of thermal axial elongations in NSOM probes have been implemented using shear-force feedback,[16] a mechanism that keeps the probe's vertical position at a relative constant distance from a sample surface.[17] Changes in the probe axial dimension are quantified by monitoring the corresponding feedback voltage signal that extends the position of the sample to avoid tip-sample crashing. The shortcoming of such a technique is its limited bandwidth (<1 kHz), which prevents the ability to identify the fast time constants that potentially might be present in thermal processes inside the probe.[18,19] This article introduces a technique of higher bandwidth. The new approach is based on the detection, in real time, of the optical interference pattern established by laser beam reflections from a Fabry–Perot type cavity formed by the flat apex of a NSOM probe and a semitransparent metal-coated glass plate. Flat-apex probe morphologies do not constitute an extra requirement for this new method to be applicable since apertured NSOM probes have indeed a well-defined cross section area at the tip end. The flat tip morphology of the probe shown in Fig. 1(a), for example, is a direct consequence of fiber cleave that occurs when a hard pull is applied to a fiber undergoing capillary instability, driven by surface tension, in the heat-pulling probe fabrication method.[20] Similarly, the flat termination in probes fabricated by chemical etching[21–23] [see Figs. 1(b) and 1(c)] results from milling the apex with a focused ion beam,[24,25] a convenient postprocedure that renders well-defined apertures. Probes used in this article were fabricated with the second method.[26]

The working principle to measure the probe axial elongation is shown in Fig. 2, where we can identify three basic components; they are: a probe-beam continuous wave laser, a pump beam serving as a periodic heat source, and an optical interference measurement setup. Notice that a Fabry–Perot type cavity results when the probe's flat apex section is placed in front of a partially transparent metal-coated glass plate. The probe and the plate are both held at fixed positions relative to the frame of a homemade NSOM microscope stage,[26] and the initial separation $d(0)$ between the cavity "mirrors" is of a few hundred micrometers. A linearly polarized He–Ne laser beam ($\lambda_1=633$ nm) is incident on the two-surface cavity, and the reflected beams establish an interference pattern in the far-field region. A pinhole selects one of the interference fringes, and the transmitted light intensity $I(0)$ is detected with a photodiode and amplified with a current preamplifier. This experimental setup allows monitoring changes in the interference pattern when the cavity length decreases as a consequence of the probe thermal elongation. As a heat source, we use a diode laser ($\lambda_2=690$ nm) to couple $\sim$0.5 mW into the tapered probe, and a laser driver of 150 kHz frequency bandwidth modulates the input power "on" and "off" (at $\sim$100 Hz) to allow repetitive measurements with a boxcar averager.[27] Upon a transition from off to on in the input power, the probe elongates and the time dependent cavity length $d=d(t)$ correspondingly produces an interference signal of intensity $I=I(t)$. The characteristic thermal time responses of the probe elongation are therefore encoded in the signal detected by the photodiode.

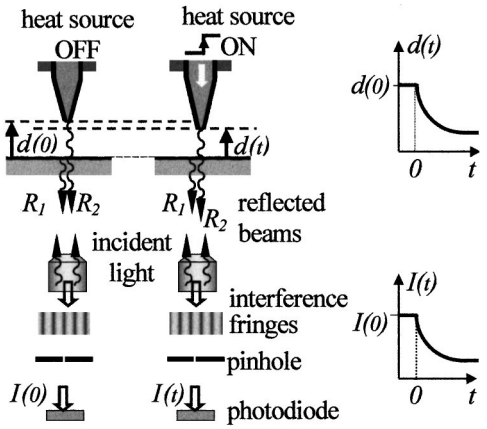

FIG. 2. Working principle to measure probe elongation, based on optical interference detection. The incident light beam reflects from both the semitransparent metal-coated glass plate ($R1$) and from the probe apex ($R2$). Both reflecting beams interfere and a pinhole selects one interference fringe whose light intensity reaches a photodiode. Thermal expansion of the probe changes the probe-plate separation distance. The probe's thermal time response is obtained from the corresponding time dependent interference signal.

We can estimate the signal level involved in these measurements from a simple model that considers the reflected beams from the cavity's two mirrors as plane waves of intensity I_1 and I_2, respectively. For a cavity separation $d=d(t)$ the signal is given by $I(d)=I_1+I_2+2\sqrt{I_1I_2}\cos[(4\pi/\lambda)d+\varphi]$, where φ accounts for any phase difference introduced by the reflections and transmissions through the mirrors. For a 10 mW light beam, focused to a spot 10 μm in diameter, incident on a probe apex of, for example, 50 nm radius, and assuming a 0.1 collection efficiency by the objective lens, intensities of the order of $\sim$100 nW, or higher, are expected to reach the photodiode. When the separation distance changes from d_0 to $d_0+\Delta d$, where $\Delta d \ll \lambda$, a Taylor's expansion in the expression for $I(d)$ earlier gives, $|\Delta I| \approx 2\sqrt{I_1I_2}(4\pi/\lambda)(\Delta d)|\sin[(4\pi/\lambda)d_0+\varphi]|$. This last expression indicates that, to a first approximation, the maximum change possible in the signal intensity, as a function of Δd, is given by

$$|\Delta I|_{\max} \approx \tilde{2}\sqrt{I_1I_2}\left(\frac{4\pi}{\lambda}\right)(\Delta d). \quad (1)$$

Expression (1) gives $\Delta I \approx 5$ nW per nm. Monitoring the probe elongation at 1 nm steps (and with a 8 kHz frequency bandwidth or greater, depending on the time resolution we are interested in) requires discriminating between the nano-

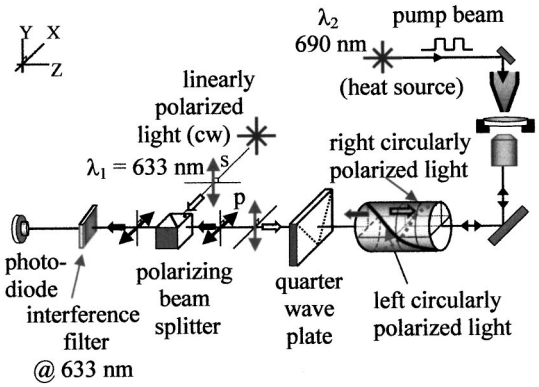

FIG. 3. Optical setup that exploits light polarization properties to reduce signal background and increase the signal to noise ratio. Light reflected from the probe-sample cavity ends up as light polarized along the *x* direction, which is the only polarization state allowed by the polarizing beam splitter to reach the photodiode.

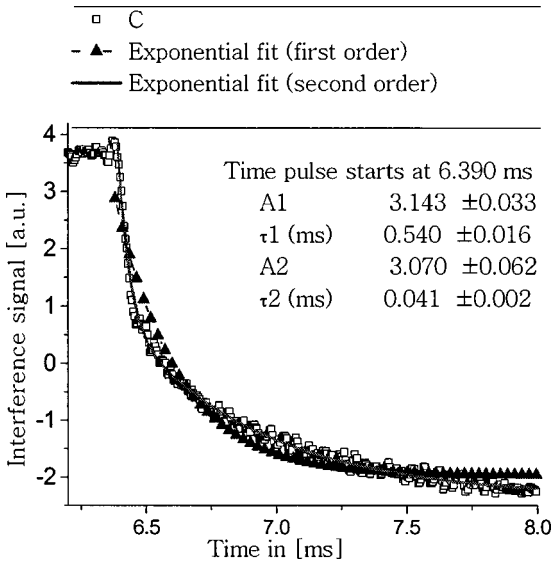

FIG. 4. Interference signal, produced by laser reflections from the probe-sample cavity, as a function of time. The probe is initially held at a fixed position and the sample-probe separation remains constant before a light pulse (from the pump beam laser) is applied at $t_0=6.39$ s. As the probe elongates the cavity length changes and so does the interference signal. The thermal time response of the probe is extracted from this curve. Notice two time constants are necessary for the fitting curve to agree with the experimental data.

watt power signal level contained in just one fringe interference and other light background reaching the photodiode. To ease this task, light polarization properties are exploited to reduce the background and improve the apparatus' detection sensitivity, as explained later.

One way to efficiently detect the interference established by the reflected beams from a cavity is to introduce a quarter wave plate and a polarizing beam splitter along the interference optical path. This is illustrated in Fig. 3. Incident light polarized along the *y* direction is fully reflected by the polarizing beam splitter and becomes a right-circularly polarized after propagating through a quarter wave plate. Reflection from either the metal-coated plate or the probe's apex produces left-circularly polarized beams that become linearly polarized along the *x* direction after passing the quarter wave plate the second time. Thus, since the beam splitter allows only light polarized along the *x* axis to reach the photodetector, which is just the type of light that results from the cavity reflections that pass through the quarter wave plate, this method achieves the goal of enhancing the signal to noise ratio, easing the task of monitoring the nanometer level probe's elongations. Furthermore, in order to reject any possible light leakage from the heat source laser, an interference filter transparent at 633 nm was used.

III. RESULTS AND DISCUSSION

During preliminary tests, changes in the cavity separation were implemented not by heating a tapered probe, but by moving the sample instead. This was accomplished by placing the sample on a piezo scanner,[27] and the interference signal was established by laser reflections from a cleaved fiber and a semitransparent metal coated glass plate. This procedure allowed precise calibration of the scanner *z* axis. A synchronized detection scheme (using a lock-in amplifier) implemented to measure the sample's vertical displacement verified 1 nm sensitivity; measurements were limited mainly by low frequency building vibrations. The signal from the photodiode was fed into a current amplifier set at 100 nA/V gain and 8 kHz bandwidth.[28] The selection of this scale had the purpose of exploring measurements of thermal elongation time responses that might be shorter than the 10 ms relaxation time associated with thermal process dominated by the probe's shank region away from the apex.[14] After completing these tests we proceeded to measure the thermal elongation time constants of tapered fibers.

Following expression (1), the time dependence of the probe elongation $\Delta d(t)$ can be obtained from the interference signal variation ΔI. Figure 4 shows the axial probe elongation as a function of time (''squares'' curve), which was obtained by averaging 150 consecutive trials. The ''triangles'' curve corresponds to a first-order exponential fit corresponding to the form $y=y_0+A\exp[-(t-t_0)/\tau_1]$, but it can be observed that the fitting is not perfect. Indeed, since many factors may influence the probe's thermal response, namely probe geometry, glass/aluminum composition and coating thickness, more than one time constant may be necessary for a more accurate description of thermal phenomena in the probe. We tried a second order exponential fit $y=y_0+A_1\exp[-(t-t_0)/\tau_1]+A_2\exp[-(t-t_0)/\tau_2]$ and the result is indicated by the solid curve, along the corresponding parameters, also in Fig. 4. The agreement with the experimental data is much better. Notice that τ_1 and τ_2 appear in the last expression with similar weight, $A_1 \approx A_2$, indicating that they are equally important. The time constants reported here, $\tau_1=(0.540\pm0.016)$ ms and $\tau_2=(0.041\pm0.002)$ ms, are much smaller than the previously reported thermal relaxation $\tau_{\text{shank}}\sim 10$ ms associated to heat diffusion across a tapered region of length $L_{\text{shank}}=\sqrt{D\tau_{\text{shank}}}\sim 200$ μm.[14] We must point out, however, that the optical setup here emphasizes the fast thermal time constants whereas the setup in Ref. 14 emphasized longer time constants. We also note that Fig. 2, in Ref. 14, shows a linear decrease of the probe's throughput signal as a function of the logarithmic values of the pulsed input

power repetition rate (a behavior not expected for a single exponential time dependence) suggesting the existence of a variety of time constants. The smaller than 10 ms time constants reported here (0.5 and 0.04 ms) are indicative that the heated region that dominates the thermal elongation process is more localized (45 and 15 μm, respectively), and, in contrast to what was observed during the measurement of τ_{shank},[14] τ_1 and τ_2 may have stronger dependence on the specific probe's geometry and coating thickness. Another consequence of the small values of τ_1 and τ_2 is that the associated diffusion lengths along the probe's axis and perpendicular to it, have a similar order of magnitude. Therefore, there is not a drastic distinction between radial and longitudinal thermalization processes; both occur at the same time, with the longitudinal one favored by the aluminum coating. Finally, our work does not rule out that large regions still may be involved in the probe's thermal process. Indeed, the absence of $\tau_{\text{shank}} \sim 10$ ms in our data can be partially explained in terms of heat diffusion along the probe axis: while heat transfer from regions of different radii results in a net contraction or elongation, at a distance 200 μm away from the apex the probes have a constant radius [see Fig. 1(b)] so a zero contribution to the net elongation is expected from that region.

The new optical technique described in this article has allowed us to measure, to the best of our knowledge, the fastest time responses associated with thermal processes in NSOM probes reported up today. The high frequency bandwidth of this new technique will enable better characterization of NSOM probes and will allow a detailed study of the physics involved in fast thermal processes affecting near-field imaging probe performance.

ACKNOWLEDGMENTS

Support of this research is by the U.S. Army Research Office through Grant No. DAAD19-01-1-0424. The authors also acknowledge useful discussions with Dr. Hans Hallen.

[1] M. A. Paesler and P. J. Moyer, *Near-Field Optics: Theory, Instrumentation and Applications* (Wiley, New York, 1996).
[2] *Near-Field Nano/Atom Optics and Technology*, edited by M. Ohtsu (Springer, Berlin, 1998).
[3] Near-Field Microscopy and Spectroscopy, edited by H. Metiu [J. Chem. Phys. **112**, 7757 (2000)].
[4] E. Betzig, J. K. Trautman, R. Wolfe, E. M. Gyorgy, P. L. Finn, M. H. Kryder, and C.-H. Chang, Appl. Phys. Lett. **61**, 142 (1992).
[5] F. Issiki, K. Ito, K. Etoh, and S. Hosaka, Appl. Phys. Lett. **76**, 804 (2000).
[6] M. L. M. Balistreri, H. Gersen, J. P. Korterik, L. Kuipers, and N. F. van Hulst, Science **294**, 1080 (2001).
[7] A. H. La Rosa, B. I. Yakobson, and H. D. Hallen, Appl. Phys. Lett. **70**, 1656 (1997).
[8] B. A. Nechay, U. Siegner, M. Achermann, H. Bielefeldt, and U. Keller, Rev. Sci. Instrum. **70**, 2758 (1999).
[9] E. Tamiya, S. Iwabuchi, N. Nagatani, Y. Murakami, T. Sakaguchi, K. Yokoyama, N. Chiba, and H. Muramatsu, Anal. Chem. **69**, 3697 (1997).
[10] J. M. Kim, T. Ohtani, S. Sugiyama, T. Hirose, and H. Muramatsu, Anal. Chem. **73**, 5984 (2001).
[11] E. Betzig and R. J. Chichester, Science **262**, 1422 (1993).
[12] R. Stockle, C. Fokas, V. Deckert, R. Zenobi, B. Sick, B. Hecht, and U. P. Wild, Appl. Phys. Lett. **75**, 160 (1999).
[13] A. Partovi *et al.*, Appl. Phys. Lett. **75**, 1515 (1999).
[14] A. H. La Rosa, B. I. Yakobson, and H. D. Hallen, Appl. Phys. Lett. **67**, 2597 (1995).
[15] G. Binnig *et al.*, Appl. Phys. Lett. **74**, 1329 (1999).
[16] P. G. Gucciardi, M. Colocci, M. Labardi, and M. Allegrini, Appl. Phys. Lett. **75**, 3408 (1999).
[17] E. Betzig, P. L. Finn, and J. S. Weiner, Appl. Phys. Lett. **60**, 2484 (1992).
[18] Measurement of fast transient signals with low frequency bandwidth instruments are reported in the literature, but the extraction of information becomes more involved. See for example, G. Nunes, Jr. and M. R. Freeman, Science **262**, 1029 (1993).
[19] It is pertinent to bring the attention of the excellent work about thermal effect in truncated metallic probes, undertaken in the context of scanning tunneling microscopy studies: V. Gerstner, A. Thon, and W. Pfeiffer, J. Appl. Phys. **87**, 2574 (2000). The findings in this article, helps to understand similar thermal phenomena occurring in NSOM probes.
[20] B. I. Yakobson, P. J. Moyer, and M. A. Paesler, J. Appl. Phys. **73**, 7984 (1993).
[21] D. R. Turner, U.S. Patent No. 4,469,554 (1984).
[22] M. N. Islam, X. K. Zhao, A. A. Said, S. S. Mickel, and C. F. Vail, Appl. Phys. Lett. **71**, 2886 (1997).
[23] P. Hoffmann, B. Dutoit, and R. Salathe, Ultramicroscopy **61**, 165 (1995).
[24] J. A. Veerman, A. M. Otter, L. Kuipers, and N. F. van Hulst, Appl. Phys. Lett. **72**, 3115 (1998).
[25] S. Pilevar, K. Edinger, W. Atia, I. Smolyaninov, and C. Davis, Appl. Phys. Lett. **72**, 3133 (1998).
[26] B. Biehler, ''Characterization of Thermal Probe Elongation in Near-Field Optical Microscopy,'' Master of science in physics thesis, Portland State University, Physics Department, 2001.
[27] A more detailed description of the equipment used in this experiment is as follows: (a) Probe beam He–Ne laser, $\lambda_1 = 633$ nm, 10 mW, continuous wave, linearly polarized; (b) photodiode S1227-1010BR, 2.29 nW/nA, from Hamamatsu; (c) current preamplifier, model SR570, from Stanford Research Systems; (d) heat source diode laser Hitachi HL6738MG, $\lambda_2 = 690$ nm, 35 mW, available from Thorlabs; (e) laser driver Thorlabs LDC500, 150 kHz bandwidth; (f) boxcar averager, model SR250 from Stanford Research Systems; (g) *XYZ* scanner equipped with capacitance sensors, Tritor-102 CAP model, from Piezosystem Jena, Inc.
[28] We tested the preamplifier time response with a light pulse. The preamp signal showed a characteristic overshoot curve response and the decay behavior closely fitted an exponential decay of 20 μs time constant.